

Robust principal graphs for data approximation

Alexander N. Gorban, Evgeny M. Mirkes, and Andrei Zinovyev

Abstract Revealing hidden geometry and topology in noisy data sets is a challenging task. An Elo-Elastic principal graph is a computationally efficient and flexible data approximator based on embedding a graph into the data space and minimizing the energy functional penalizing the deviation of graph nodes both from data points and from a pluri-harmonic configuration (generalization of linearity). The structure of the principal graph is learned from data by application of a topological grammar which in the simplest case leads to the construction of principal curves or trees. In order to more efficiently cope with noise and outliers, we suggest using a trimmed data approximation term to increase the robustness of the method. The modification of the method that we suggest does not affect either computational efficiency or general convergence properties of the original elastic graph method. The trimmed elastic energy functional remains a Lyapunov function for the optimization algorithm. On several examples of complex data distributions we demonstrate how the robust principal graphs learn the global data structure and show the advantage of using the trimmed data approximation term for the construction of principal graphs and other popular data approximators.

Alexander N. Gorban and Evgeny M. Mirkes
Department of Mathematics, University of Leicester, Leicester, LE1 7RH, UK,
✉ ag153@le.ac.uk, em322@le.ac.uk

Andrei Zinovyev
Institut Curie, 26 rue d'Ulm, Paris 75248, France,
✉ andrei.zinovyev@curie.fr

ARCHIVES OF DATA SCIENCE (ONLINE FIRST)
KIT SCIENTIFIC PUBLISHING
Vol. 2, No. 1, 2017

DOI 10.5445/KSP/1000058749/11
ISSN 2363-9881



1 Introduction

In this paper, we consider a classical problem: How to approximate a finite set D in R^m for relatively large m by a finite subset of regular low-dimensional objects in R^m . In applications this problem arises in many areas: From data visualization (e.g., visualization of the differences between human genomes) to fluid dynamics.

A typical data approximation task starts with the following question: Is the dataset D situated near a low-dimensional affine manifold (plane) in R^m ? If we look for a point, straight line, plane, ... that minimizes the average squared distance to the datapoints, we immediately come to the Principal Component Analysis (PCA) which is one of the most seminal inventions in data analysis (Jolliffe, 2002). The nonlinear generalization of PCA remains a challenging task. One of the earliest attempts suggested in this direction was the Self-Organizing Map (SOM) (Kohonen, 2001) with its multiple generalizations and implementations such as Growing SOM (GSOM) (Alahakoon et al, 2000). However, unlike classical PCA and k -means, the SOM algorithm is not based on optimization of any explicit functional (Erwin et al, 1992).

For a known probability distribution, *principal manifolds* were introduced as lines or surfaces passing through “the middle” of the data distribution (Hastie and Stuetzle, 1989). Several algorithms for the construction of principal curves (Kégl and Krzyżak, 2002) and surfaces for finite datasets were developed during the last decade, as well as many applications of this idea. In the end of 1990s, a method of multidimensional data approximation based on elastic energy minimization was proposed (see (Gorban’ and Rossiev, 1999; Zinovyev, 2000; Gorban and Zinovyev, 2005, 2001; Gorban et al, 2008a; Gorban and Zinovyev, 2009) and the bibliography there). This method is based on the analogy between the principal manifold and the elastic membrane. Following the metaphor of elasticity, two quadratic regularization terms are introduced which penalize the non-smoothness of data approximators. This allows one to apply the standard expectation-minimization strategy with a quadratic form of the optimized functionals at the minimization step (i.e., solving a system of linear algebraic equations with a sparse matrix). Later on, the elastic energy was applied to constructing principal elastic graphs (Gorban et al, 2007). A related idea of optimizing the elastic energy of a system of springs representing the graph embedding in low-dimensional spaces was previously used in the de-

velopment of graph drawing algorithms (Fruchterman and Reingold (1991); Kobourov (2012)).

The method of elastic energy minimization allows creating analogs of SOM (Kohonen, 1982) and neural gas (Martinetz et al, 1993) with an explicit functional to minimize: The elastic map is an analog of SOM and the principal graph is an analog of a neural gas. The main advantage of optimization-based analogs is the ability to explicitly control for smoothness (or other types of regularity, such as harmonicity) of data approximators.

However, the main drawback of all described methods of approximation is sensitivity to outliers and noise, which is caused by the very nature of Euclidean distance (or quadratic variance): data points distant to the approximator have very large relative contributions. There exist several widely used ideas for increasing an approximator's robustness in the presence of strong noise in data such as substituting the Euclidean norm by the L_1 norm (e.g. Ding et al (2006); Hauberg et al (2014)) and outliers exclusion or fixed weighting or iterative reweighting during the construction of data approximators (e.g. Xu and Yuille (1995); Allende et al (2004); Kohonen (2001)). In some works, it was suggested to utilize "trimming" averages, e.g. in the context of the k -means clustering or some generalizations of PCA (Cuesta-Albertos et al (1997); Hauberg et al (2014)).

The general idea of trimming consists in penalizing the contribution of data points distant from the mean to the estimation of variance. In the simplest scenario the points that are too distant from the mean are completely neglected; in more complex scenarios the distant points contribute less than the close ones. This way of robustification probably goes back to the notion of a truncated (or trimmed) mean by Huber (1981). The strategy of trimming can be used in the construction of SOMs, elastic maps or almost any other data approximators.

2 Graph grammars and elastic principal graphs

For a description of the basic algorithms we refer to (Gorban et al, 2007). More explanatory materials including the pseudo-codes can be found online¹.

Let G be a simple undirected graph with a set of vertices Y and set of edges E . For $k \geq 2$ a k -star in G is a subgraph with $k + 1$ vertices $y_{0,1,\dots,k} \in Y$ and k edges $\{(y_0, y_i) \mid i = 1, \dots, k\} \subset E$. Suppose for each $k \geq 2$, a set of S_k of k -stars

¹ <https://github.com/auranic/Elastic-principal-graphs/wiki>

in G (subgraphs) has been selected. We call a graph G with selected families of k -stars S_k an *elastic graph* if, for all $E^{(i)} \in E$ and $S_k^{(j)} \in S_k$, the correspondent elasticity moduli $\lambda_i > 0$ and $\mu_{kj} > 0$ are defined. Let $E^{(i)}(0), E^{(i)}(1)$ be vertices of an edge $E^{(i)}$ and $S_k^{(j)}(0), \dots, S_k^{(j)}(k)$ be vertices of a k -star subgraph $S_k^{(j)}$ (among them, $S_k^{(j)}(0)$ is the central vertex). For any map $\phi : Y \rightarrow R^m$ the *energy of the graph* is defined as

$$U^\phi(G) := \sum_{E^{(i)}} \lambda_i \left\| \phi(E^{(i)}(0)) - \phi(E^{(i)}(1)) \right\|^2 + \sum_{S_k^{(j)}} \mu_{kj} \left\| \phi(S_k^{(j)}(0)) - \frac{1}{k} \sum_{i=1}^k \phi(S_k^{(j)}(i)) \right\|^2. \quad (1)$$

For a given map $\phi : Y \rightarrow R^m$ we divide the dataset D into node neighborhoods $K^y, y \in Y$. The set K^y contains the data points for which the node $\phi(y)$ is the closest one in $\phi(Y)$. The *energy of approximation* is:

$$U_A^\phi(G, D) = \frac{1}{\sum_x w(x)} \sum_{y \in Y} \sum_{x \in K^y} w(x) \|x - \phi(y)\|^2, \quad (2)$$

where $w(x) \geq 0$ are the point weights. A simple and fast algorithm for minimization of the energy

$$U^\phi = U_A^\phi(G, D) + U^\phi(G) \quad (3)$$

is the splitting algorithm, in the spirit of the classical k -means clustering: For a given system of sets $\{K^y \mid y \in Y\}$ we minimize U^ϕ (optimization step, it is the minimization of a positive quadratic functional), then for a given ϕ we find new a $\{K^y\}$ (re-partitioning), and so on. Stop when no change occurs.

In practice the structure and complexity of the optimal graph for the approximation of a complex dataset is not known. To learn it from the data, the principal elastic graphs are constructed using a growing schema. All possible graph structures are defined by a graph grammar. The optimal graph structure is obtained by the sequential application of graph grammar operations to the simplest initial graph (Gorban et al, 2007). A link in the energetically optimal transformation chain is added by finding a transformation application that gives the largest energy descent (after an optimization step). Then the next link is added, and so on, until we achieve the desirable accuracy of approximation, or

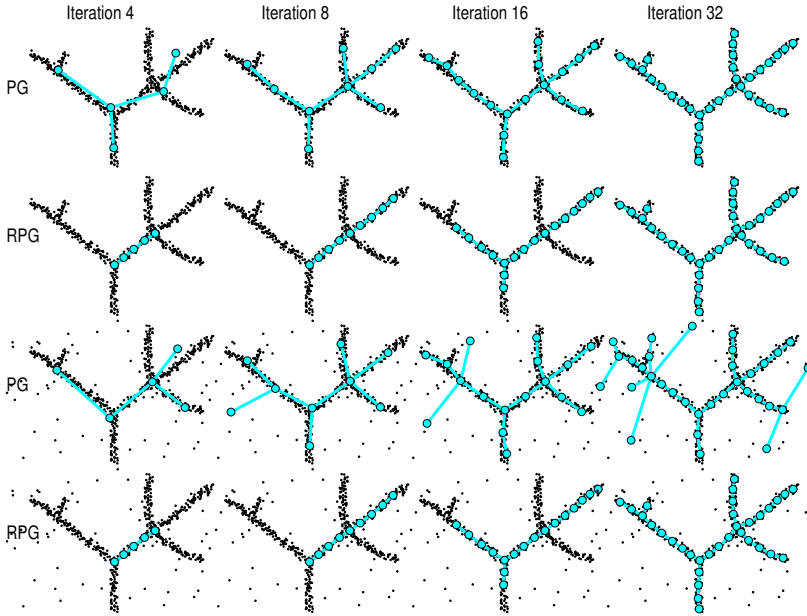


Fig. 1: Examples of principal graph (PG) and robust principal graph (RPG) construction for: clear (two top rows) and noisy (two bottom rows) data patterns

the limit number of transformations. Other termination criteria are also possible (Zinovyev and Mirkes, 2013)).

As simple (but already rather powerful) example we use a system of two transformations: “add a node to a node” and “bisect an edge”. These transformations act on a class of *primitive elastic graphs*: all non-terminal nodes with k edges are centers of elastic k -stars, which form all the k -stars of the graph. This grammar produces *elastic principal trees*, i.e. graphs having no loops.

3 Robust elastic principal graphs

In order to introduce the robust elastic principal graphs, we consider the motivating toy problem of learning a complex one-dimensional pattern sampled by points densely located around. The pattern can be accompanied by a background noisy, relatively sparse and stochastic distribution of points not con-

nected to the pattern (see fig. 1). The top row in fig. 1 shows several steps of the elastic principal graph construction in the case of absence of noise. From the fig. 1, third row, it is clear that the presence of background noise can completely distort the resulting principal graph, introducing excessive branching in order to capture the variance of the noise points located distantly from the pattern.

Here we apply a particular variant of “impartial trimming” (Gordaliza, 1991) or “data-driven trimming” suitable for principal graphs. We introduce a parameter R_0 (called “robustness radius”) which specifies what is the maximal distance from a node of the principal graph at which a data point can affect the position of the node during the current iteration of the energy optimization process. We require that all the data points which are more distant than R_0 from any graph node, do not contribute to the gradient of the optimized functional U^ϕ . However, they have a constant non-zero contribution R_0^2 to the value of the data approximation term which is required for preserving the properties of the optimized functional U^ϕ to be a Lyapunov function (see sec. 4 and fig. 2).

In order to satisfy these requirements, we have to change the data approximation energy term only, because $U^\phi(G)$ term is independent of the data. The data-dependent approximation energy term eg.(2) is modified as follow:

$$U_R^\phi(G, D) = \frac{1}{\sum_x w(x)} \sum_{y \in Y} \sum_{x \in K^y} w(x) \min\{\|x - \phi(y)\|^2, R_0^2\}, \quad (4)$$

where R_0 is the robustness radius. All other terms in the energy function are the same: $U^\phi = U_R^\phi(G, D) + U^\phi(G)$. It means that all optimization strategies used for the construction of principal graphs are applicable for robust principal graphs too, and that the optimization problem remains quadratic at the node optimization step. Notice that eg. (4) can be re-written as

$$U_R^\phi(G, D) = \frac{1}{\sum_x w(x)} \sum_{y \in Y} \sum_{x \in K^y, \|x - \phi(y)\| < R_0} w(x) \|x - \phi(y)\|^2 + \quad (5)$$

$$+ \frac{1}{\sum_x w(x)} \sum_{\|x - \phi(y)\| \geq R_0, \forall y} w(x) R_0^2,$$

From this it becomes evident that the second term is constant and does not contribute to the derivative U'_y .

The result of such a modification is shown in fig. 1, second and fourth rows. A robust principal graph learns the data for a local fragment and traces the local data structure, branching if this is energetically optimal. As a result, the global

structure of the data distribution is detected only at the end of graph growth and only if there are no gaps in the data distribution larger than the robustness radius R_0 .

4 Convergence of robust elastic principal graphs

Adding trimming to the data approximation term as in eq. (4) does not change the property of the elastic principal graph's energy to converge to a local energy minimum. Both energy functions, the one defined by eq. (3) and the robust one

$$U = \frac{1}{\sum_x w(x)} \sum_{y \in Y} \sum_{x \in K^y} w(x) \min\{\|x - \phi(y)\|^2, R_0^2\} + U^\phi(G) \quad (6)$$

are Lyapunov functions for the splitting-based optimization algorithm used for constructing the elastic principal graphs. The existence of a Lyapunov function guarantees convergence of the optimization algorithm based on the splitting schema.

Let us formally demonstrate that at each step of the optimization splitting algorithm, the energy (6) does not increase.

Each graph optimization algorithm step is split into two parts. First, with fixed partitioning of the dataset D into graph node neighbourhoods $K^y, y \in Y$, the quadratic function (6) is minimized which leads to the new positions of the nodes $\phi'(y)$. At this step, the energy U can not increase because it is minimized: $U(\phi'(y)) \leq U(\phi(y))$.

Secondly, a new partitioning into sets $K^{y'}$ of data points x is computed with respect to the new positions of the nodes $\phi'(y)$. Let us denote by K_c^y the set of points from K^y which are not more distant than R_0 from $\phi(y)$: $K_c^y = \{x \mid \|\phi(y) - x\| \leq R_0\}$, and let us denote the set of "distant" points as $K_f^y = \{x \mid \|\phi(y) - x\| > R_0\}$. Of course, the whole neighbourhood is a union of these two sets, and their intersection is empty: $K^y = K_c^y \cup K_f^y$. After the new partitioning, we will have a new $K^{y'} = K_c^{y'} \cup K_f^{y'}$. Let us consider one particular neighbourhood K^{y_1} and any other one K^{y_2} . During the first step, $\phi(y_1) \rightarrow \phi'(y_1)$ and $\phi(y_2) \rightarrow \phi'(y_2)$. After re-partitioning, we have four possible re-assignments of a data point $x \in K^{y_1}$ (see Figure 2):

1. $K^{y_1} \rightarrow K^{y_1}$: In this case the energy $U_R^\phi(G, D)$ does not change since the point x remains in the neighbourhood of y_1 .

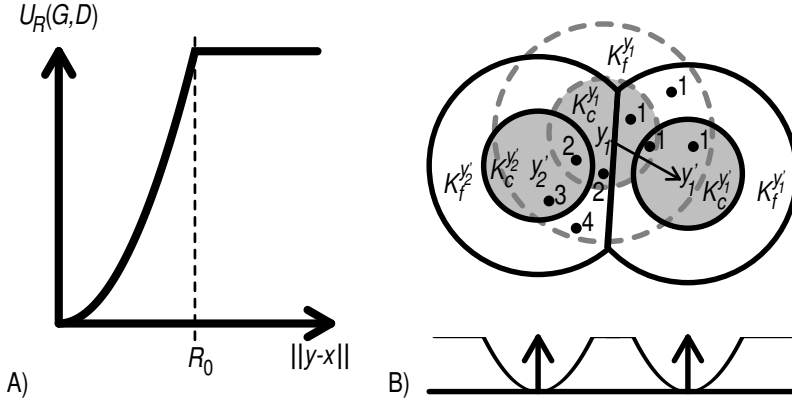


Fig. 2: A) The functional form of the trimmed approximation energy term. B) Possible re-partitioning of the data points (only several of them are shown as black circles with numbers) belonging to K^{y_1} after changing the node position at the graph optimisation step. Four possible cases (1-4) are shown, and each one leads to non-increasing approximation energy (see text for explanation). Here the shaded area denotes the robustness radius R_0 for a graph node, the big solid circle denotes the neighbourhood K^{y_1} . The neighbourhood K^{y_1} is split into “close” points $K_c^{y_1}$ and “distant” points $K_f^{y_1}$.

2. $K_c^{y_1} \rightarrow K^{y_2}$: In this case the energy term related to the node y_2 in $U_R^\phi(G, D)$ decreases because by the definition of a neighbourhood $\|\phi'(y_1) - x\| > \|\phi'(y_2) - x\|$.

3. $K_f^{y_1} \rightarrow K_c^{y_2}$: In this case the energy term related to the node y_2 in $U_R^\phi(G, D)$ will not increase because it will change from R_0^2 to $\|\phi'(y_2) - x\|^2 \leq R_0^2$.

4. $K_f^{y_1} \rightarrow K_f^{y_2}$: In this case the energy term related to the node y_2 in $U_R^\phi(G, D)$ does not change (it equals R_0^2 before and after re-partitioning).

The same four scenarios are valid for any pair $y_i \neq y_j$. Therefore, the total energy $U_R^\phi(G, D)$ can not increase while $U^\phi(G)$ is not affected by re-partitioning. It is also clear that the non-negativity of the derivative of the trimmed approximation energy function (Figure 2A) is essential that U does not increase, because otherwise case (3) can lead to an increase of $U_R^\phi(G, D)$. For example, disregarding the contribution of “distant” points for their contribution to the approximation of energy completely would lead to a violation of property (3).

5 Comparing various types of robust and non-robust data approximators

Let us further exploit the benefits that trimming the data approximation term can bring to approximating complex toy 2D patterns. Fig. 3 shows the results of application of the standard and the robust versions of SOM, elastic maps and principal graphs for spiral and kappa-like data 2D patterns. 10% of noise is introduced into the data distribution, e.g. the fraction of randomly positioned points not belonging to the data pattern is 0.1 of the number of points in the pattern. For robustification of the non-batch SOM, specific methods were used as described in Allende et al (2004) and Kohonen (2001). All robust versions in case of methods use the same robustness radius. For all methods, robustification of approximators led to more exact approximation of the data pattern.

6 Application of robust graphs to the data on human genome diversity

The Human Genome Diversity Project (HGDP) collected a large collection of single nucleotide polymorphism (SNP) genotype profiles capturing the major sources of variation between human genomes. The publicly available HGDP dataset which can be downloaded from <http://www.hagsc.org/hgdp/files.html> contains samples of 53 historically native populations from 7 large geographical regions (Africa, Near East, Europe, South Central Asia, East Asia, America, Oceania). Each of the 1043 individuals in this dataset is represented by a profile of 660 918 SNPs. It was demonstrated before that the dataset shows non-trivial branching structure reflecting the combined effect of migration and adaptation of humanity in various geographical conditions (Elhaik et al, 2014). Therefore, it is interesting to approximate this dataset by an optimally branching approximator such as the principal tree.

In order to represent the dataset as a set of numerical vectors in a multidimensional space, we've applied the standard SNP quantification approach. For each row of the table corresponding to a particular SNP, the homozygous status of the SNP was coded as '0', while two different heterozygous statuses were assigned '-1' and '+1'. All unreliably measured SNP statuses were filtered out, which resulted in a numerical table of 1043 individuals (objects) and 429 830 SNPs (variables). At first, we have reduced the dimension of the dataset to R^3

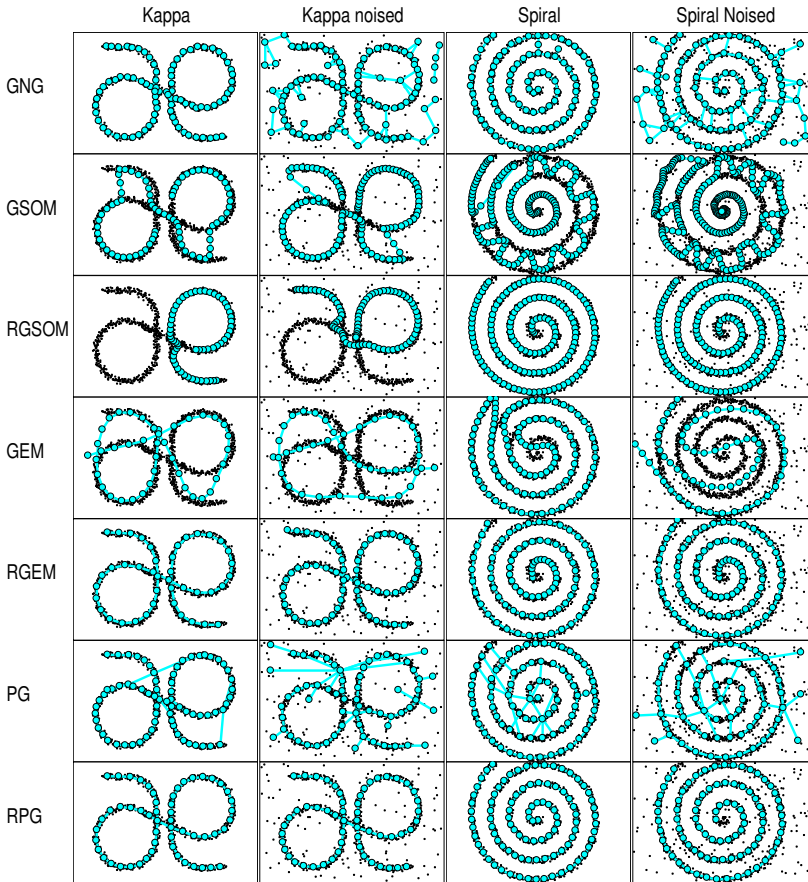


Fig. 3: Examples of different data approximator performances for four 2D toy complex patterns: from left to right: clear kappa-like, noised kappa-like, clear spiral, noised spiral; from top to bottom: Growing Neural Gas (GNG)(Martinetz et al, 1993), Growing SOM (GSOM) and Robust GSOM (RGSOM) (Alahakoon et al, 2000), growing elastic map (GEM), robust GEM (RGEM), principal graph (PG)(Gorban et al, 2007; Gorban and Zinovyev, 2009), and robust principal graph (RPG).

by applying a standard principal component analysis (PCA). In this reduced space we have constructed both standard and robust versions of principal trees.

Application of the standard principal trees was not successful due to their inability to capture fine local details of the data distribution (the figures can be found online²), which resulted in mixing up the native populations belonging to the same region. For example, all variants of the European population were mapped to a single tree node. Changing the elasticity parameters did not improve the situation.

At the same time, application of the robust principal trees with an initialization from two points belonging to a local neighborhood resulted only in a local description of the variety of human genomes. This was probably due to the fact that the distribution of individuals is characterized by certain gaps not covered by 1043 genomes (and which could probably represent non-existent parts of human genome diversity).

Therefore, it was not possible to find a combination of parameters which could represent both global and local patterns of the branching distribution of human genomes. However, we could significantly improve the result by application of a hybrid approach. We trained the principal tree in two epochs. During the first epoch, non-robust principal graphs were applied to outline the general features of the global structure of the dataset, representing roughly the global relations between geographical regions. By contrast, during the second epoch, the robust principal tree approach was applied starting from the principal tree configuration obtained at the first step. During the second stage, the elasticity coefficients of the principal tree were significantly reduced in order to achieve a better local approximation of the data. As a result, the constructed principal tree was able to capture the global pattern of genomic diversity between geographical regions and the local patterns of genomic diversity between native sub-populations of the same region. For example, Russian, Italian, Sardinian, Orcadian, Druze, Basque, Kalash populations were mapped to their own nodes (see fig. 4), resolving the structure of genomic diversity at a higher level of detail.

In order to represent the principal tree on a 2D plane we used the previously described metro map layout of a tree on the plane (Gorban et al, 2008b; Gorban and Zinovyev, 2010). This layout is constructed in order to represent the harmonical nature of the embedding of a principal tree into multidimensional space in the best fashion. The center of each star of the tree is the mean point

² <http://goo.gl/CbFMIC>

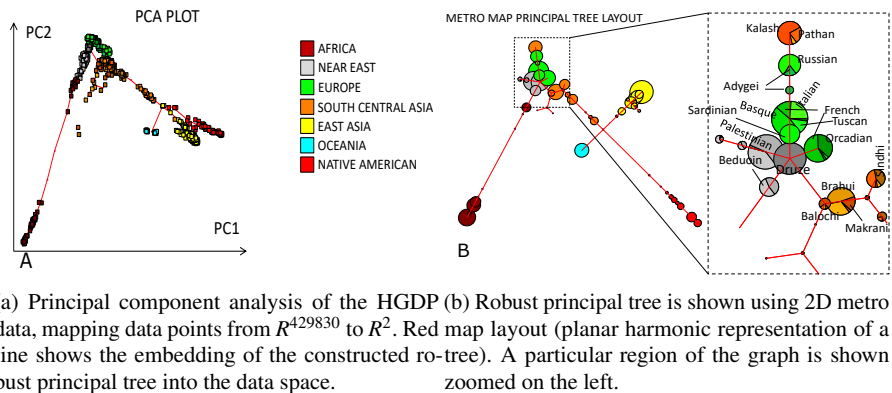
of the set of the star's leaves (see fig. 4B). The number of individuals from distinct populations mapped to the same tree node were represented as a pie-chart diagram (fig. 4B). The distances between tree nodes in 2D represent approximately the edge lengths in the multidimensional space, therefore, it is possible to estimate which populations are more distinct than others. For example, in the 2D PCA plot the composition of native american SNPs seems similar to the composition asian populations (fig. 4A). Unfortunately this is not the case. However, from the metro map layout (fig. 4B) it is clear that the composition of SNPs of native Americans is significantly different from the one of Asian populations, even more distinct the SNP profiles of population of Oceania. Interestingly, a part of East Asian populations (Kalashs and Pathans) was mapped closer to the European populations than the rest of East Asia. Indeed, there exists a controversial discussion of whether Kalash and Pathan populations living in Pakistan have European roots (e.g., originated from the troops of Alexander the Great) (Firasat et al, 2007; Wood, 2001). Here we can not make any strong conclusion regarding this point. However, construction of principal trees could potentially contribute to discussions.

To conclude, we can observe that introducing robust principal trees in the analysis of genomic data allows better tracing the local patterns in complex real-life data distributions.

7 Implementation details and computational protocols

All 2D illustrations used in this paper are created by a Java applet, developed by the authors, for constructing non-linear approximations of 2D data, using various algorithms described in (Mirkes, 2011). The construction of principal graphs in multidimensional space was performed using the VDAOEngine Java library developed by the authors. The Parameters of the methods used are provided together with the code from the corresponding GitHub page³.

³ <https://github.com/auranic/Elastic-principal-graphs/wiki/Robust-principal-graphs>



(a) Principal component analysis of the HGDP data, mapping data points from R^{429830} to R^2 . (b) Robust principal tree is shown using 2D metro data, mapping data points from R^{429830} to R^2 . Red map layout (planar harmonic representation of a line) shows the embedding of the constructed ro-tree). A particular region of the graph is shown zoomed on the left.

Fig. 4: Constructing a robust principal tree for the dataset mapping human genome diversity measured by single nucleotide polymorphism (SNP) genome-wide profiles (HGDP dataset). Large geographical regions are presented by a color while various tints of the color represent the distinct native populations within a region (only variability of European, Near East and part of South Central Asia is shown by aspects of the same color).

8 Conclusion and Summary

We described our implementation of a robust version of a principal elastic graph algorithm which is based on trimming the data approximation term in the elastic energy equation of the graph. Growing principal graphs proceeds by approximation of local data structures and tracing them till the global structure is detected. For those data distributions which contain several isolated clusters, it is necessary to restart robust principal graphs several times (one graph for each cluster) or apply a hybrid approach as described in this paper. The algorithm contains an additional parameter R_0 which is called the robustness radius. Only the data points inside this radius around a graph node y can influence position of y at the next iteration step. The algorithm shows good performance in the case when the global data structure is spoiled by a noisy background distribution of data points, which makes the algorithm more suitable in many practical applications (such as image recognition). The existence of for Lyapunov function guarantees convergence of the optimization algorithm based on the splitting schema.

The suggested data trimming method can be applied for other data approximators such as elastic maps and SOMs. In the future, we plan to apply the recently suggested machine learning framework (piece-wise quadratic based optimization of sub-quadratic growth PQSQ-based optimization) to introduce a piece-wise quadratic form of the data approximation term which will allow taking into account the position of distant data points with smaller weights and avoid the problem of defining the robustness radius (Gorban et al, 2016).

References

- Alahakoon D, Halgamuge SK, B S (2000) Dynamic self-organizing maps with controlled growth for knowledge discovery. *IEEE Transactions on Neural Networks* 11(3):601–614, DOI 10.1109/72.846732
- Allende H, Moreno S, Rogel C, Salas R (2004) Robust self-organizing maps. In: *Progress in Pattern Recognition, Image Analysis and Applications, Lecture Notes in Computer Science*, vol. 3287, Springer, pp 179–186, DOI 10.1007/978-3-540-30463-0_22
- Cuesta-Albertos J, Gordaliza A, Matrán C, et al (1997) Trimmed k -means: An attempt to robustify quantizers. *The Annals of Statistics* 25(2):553–576, DOI 10.1214/aos/1031833664
- Ding C, Zhou D, He X, Zha H (2006) R1-PCA: rotational invariant L1-norm principal component analysis for robust subspace factorization. *Proceedings of the 23 rd International Conference on Machine Learning*, Pittsburgh, PA, 2006 pp 281–288, DOI 10.1145/1143844.1143880
- Elhaik E, Tatarinova T, Chebotarev D, Piras IS, Maria Calò C, De Montis A, Atzori M, Marini M, Tofanelli S, Francalacci P, Pagani L, Tyler-Smith C, Xue Y, Cucca F, Schurr TG, Gaieski JB, Melendez C, Vilar MG, Owings AC, Gómez R, Fujita R, Santos FR, Comas D, Balanovsky O, Balanovska E, Zalloua P, Soodyall H, Pitchappan R, Ganeshprasad A, Hammer M, Matisoo-Smith L, Wells RS, GC (2014) Geographic population structure analysis of worldwide human populations infers their biogeographical origins. *Nat Commun* 5:3513, DOI 10.1038/ncomms4513
- Erwin E, Obermayer K, Schulten K (1992) Self-organizing maps: ordering, convergence properties and energy functions. *Biological Cybernetics* 67(1):47–55, DOI 10.1007/BF00201801

- Firasat S, Khaliq S, Mohyuddin A, Papaioannou M, Tyler-Smith C, Underhill PA, Ayub Q (2007) Y-chromosomal evidence for a limited greek contribution to the pathan population of pakistan. *Eur J Hum Genet* 15(1):121–126, DOI 10.1038/sj.ejhg.5201726
- Fruchterman TM, Reingold EM (1991) Graph drawing by force-directed placement. *Software: Practice and experience* 21(11):1129–1164, DOI 10.1002/spe.4380211102
- Gorban' A, Rossiev A (1999) Neural network iterative method of principal curves for data with gaps. *Journal of Computer and Systems Sciences International (c/c of Tekhnicheskaja Kibernetika)* 38:825–830
- Gorban A, Zinovyev A (2001) Visualization of data by method of elastic maps and its applications in genomics, economics and sociology. ITHES Preprints URL <http://preprints.ihes.fr/M01/Resu/resu-M01-36.html>
- Gorban A, Zinovyev A (2005) Elastic principal graphs and manifolds and their practical applications. *Computing* 75(4):359–379, DOI 10.1007/s00607-005-0122-6
- Gorban A, Mirkes E, Zinovyev A (2016) Piece-wise quadratic approximations of arbitrary error functions for fast and robust machine learning. *Neural Networks*, in press DOI 10.1016/j.neunet.2016.08.007, URL <https://arxiv.org/abs/1605.06276>
- Gorban AN, Zinovyev AY (2009) Principal graphs and manifolds. In: Olivas ES, Guerrero JDM, Sober MM, Benedito JRM, López AJS (eds) *Handbook of Research on Machine Learning Applications and Trends: Algorithms, Methods, and Techniques*, Hershey – New York. IGI Global, pp 28–59, DOI 10.4018/978-1-60566-766-9
- Gorban AN, Zinovyev AY (2010) Principal manifolds and graphs in practice: from molecular biology to dynamical systems. *International Journal of Neural Systems* 20(3):219–232, DOI 10.1142/S0129065710002383
- Gorban AN, Sumner NR, Zinovyev AY (2007) Topological grammars for data approximation. *Applied Mathematics Letters* 20(4):382–386, DOI 10.1016/j.aml.2006.04.022
- Gorban AN, Kégl B, Wunsch DC, Zinovyev AY (eds) (2008a) *Principal Manifolds for Data Visualisation and Dimension Reduction*. Lecture Notes in Computational Science and Engineering, Vol. 58, Springer, Berlin
- Gorban AN, Sumner NR, Zinovyev AY (2008b) Beyond the concept of manifolds: Principal trees, metro maps, and elastic cubic complexes. In: *Principal Manifolds for Data Visualization and Dimension Reduction*, Springer, Berlin, pp 219–237, DOI 10.1007/978-3-540-73750-6_9

- Gordaliza A (1991) Best approximations to random variables based on trimming procedures. *Journal of Approximation Theory* 64(2):162–180, DOI 10.1016/0021-9045(91)90072-I
- Hastie T, Stuetzle W (1989) Principal curves. *Journal of the American Statistical Association* 84(406):502–516, DOI 10.1080/01621459.1989.10478797
- Hauberg S, Feragen A, Black MJ (2014) Grassmann averages for scalable robust PCA. In: *Computer Vision and Pattern Recognition (CVPR), 2014 IEEE Conference on, IEEE*, pp 3810–3817, DOI 10.1109/CVPR.2014.481
- Huber P (1981) *Robust Statistics*. Wiley, New York, DOI 10.1002/0471725250
- Jolliffe I (2002) *Principal component analysis*. Springer Series in Statistics, Springer, New York, DOI 10.1007/b98835
- Kégl B, Krzyżak A (2002) Piecewise linear skeletonization using principal curves. *IEEE Transactions on Pattern Analysis and Machine Intelligence* 24(1):59–74, DOI 10.1109/34.982884
- Kobourov SG (2012) Spring embedders and force directed graph drawing algorithms. CoRR abs/1201.3011, URL <http://arxiv.org/abs/1201.3011>
- Kohonen T (1982) Self-organized formation of topologically correct feature maps. *Biological Cybernetics* 43(1):59–69, DOI 10.1007/BF00337288
- Kohonen T (2001) *Self-organizing Maps*. Springer Series in Information Sciences, Vol.30, Springer, Berlin, DOI 10.1007/978-3-642-56927-2
- Martinetz TM, Berkovich SG, Schulten KJ (1993) Neural-gas’ network for vector quantization and its application to time-series prediction. *IEEE Transactions on Neural Networks* 4(4):558–569, DOI 10.1109/72.238311
- Mirkes E (2011) Applet for constructing non-linear approximations of 2d data, using various algorithms. URL <http://bioinfo-out.curie.fr/projects/elmap/applet/Master.htm>
- Wood M (2001) *In the footsteps of Alexander the Great: a journey from Greece to Asia*. Univ of California Press, Oakland
- Xu L, Yuille A (1995) Robust principal component analysis by self-organizing rules based on statistical physics approach. *IEEE Transactions on Neural Networks* 6(1):121–143, DOI 10.1109/72.363442
- Zinovyev A (2000) *Vizualizatsiya mnogomernykh dannykh (Visualization of Multidimensional Data)*. Krasnoyarsk State Technical University, Krasnoyarsk
- Zinovyev A, Mirkes E (2013) Data complexity measured by principal graphs. *Computers & Mathematics with Applications* 65(10):1471–1482, DOI [Datacomplexitymeasuredbyprincipalgraphs](https://doi.org/10.1016/j.camwa.2013.07.011)